

Molecular dynamics simulations of EXAFS in germanium

Research Article

Janis Timoshenko*, Alexei Kuzmin[†], Juris Purans[‡]

*Institute of Solid State Physics, University of Latvia,
Kengaraga street 8, LV-1063, Riga, Latvia*

Received 22 June 2010; accepted 11 August 2010

Abstract: Classical molecular dynamics simulations have been performed for crystalline germanium with the aim to estimate the thermal effects within the first three coordination shells and their influence on the single-scattering and multiple-scattering contributions to the Ge K-edge extended x-ray absorption fine structure (EXAFS).

PACS (2008): 61.05.cj, 78.70.Dm, 02.70.Ns

Keywords: germanium • EXAFS • molecular dynamics • multiple-scattering
© Versita Sp. z o.o.

1. Introduction

The accurate analysis of the Ge K-edge extended x-ray absorption fine structure (EXAFS) in germanium is a long standing problem due to the presence of multiple-scattering (MS) contributions, which strongly influences the “classical” EXAFS analysis based on the single-scattering (SS) approach [1]. Our previous analysis [2] of thermal effects in the two isotopes of ⁷⁰Ge and ⁷⁶Ge within the first three coordination shells has been performed using both SS and MS models. We found that while the ratio of the Einstein frequencies for the second and third shells agrees well for the two models, the absolute values of Einstein frequencies are slightly overestimated in the

SS model [2]. Unfortunately, the conventional MS EXAFS analysis is limited by two factors: the simplified description of thermal effects within the MS model and a large number of correlated model parameters required.

In this work we present for the first time the classical molecular dynamics (MD) simulation of the Ge K-edge EXAFS using recently developed approach [3].

2. Simulation details

The configuration-averaged Ge K-edge EXAFS spectra for crystalline germanium were simulated at required temperatures by a two step procedure developed in [3]. First, a set of instantaneous atomic configurations was obtained from the molecular dynamics simulation, using the proper force-field potential model [4–7]. Next, the EXAFS spectra were calculated within the MS approach for each instantaneous atomic configuration and averaged to obtain the

*E-mail: timoshenkojanis@inbox.lv (Corresponding author)

[†]E-mail: a.kuzmin@cfi.lu.lv

[‡]E-mail: purans@cfi.lu.lv

configuration-averaged EXAFS signal. The latter can be directly compared with the experimental EXAFS data [3]. The MD simulations were performed by the GULP3.1 code [8] in the NVT ensemble at several temperatures on 5x5x5, 6x6x6, 7x7x7, and 8x8x8 supercells of the diamond-type (space group $Fd\bar{3}m$) germanium containing 250, 432, 686, and 1024 Ge atoms, respectively. The simulations performed with different supercell sizes gave close results, therefore the smallest supercell 5x5x5 was used in most simulations to save computing resources.

The interaction between germanium atoms was modeled by the two force-fields: Tersoff [4] and Stillinger-Weber (SW) [5–7]. They include both two and three atom interactions and are described below.

The Tersoff force-field model is defined as [4]

$$V(r_1, r_2, \dots, r_n, \Theta_1, \Theta_2, \dots, \Theta_m) = \sum_i V_i = \frac{1}{2} \sum_{i \neq j} V_{ij},$$

$$V_{ij} = f_C(r_{ij}) [a_{ij} f_R(r_{ij}) + b_{ij} f_A(r_{ij})],$$

$$a_{ij} = (1 + \alpha^n \eta_{ij}^n)^{-\frac{1}{2n}},$$

$$b_{ij} = (1 + \beta^n \zeta_{ij}^n)^{-\frac{1}{2n}},$$

$$f_A(r) = -B \exp(-\lambda_2 r),$$

$$f_R(r) = A \exp(-\lambda_1 r),$$

$$f_C(r) = \begin{cases} 1, & r < R - D \\ \frac{1}{2} - \frac{1}{2} \sin\left(\frac{\pi}{2} \frac{r-R}{D}\right), & R - D < r < R + D \\ 0, & r > R + D \end{cases},$$

$$\eta_{ij} = \sum_{k \neq i, j} f_C(r_{ij}) \exp\left[\lambda_3^3 (r_{ij} - r_{jk})^3\right],$$

$$\zeta_{ij} = \sum_{k \neq i, j} f_C(r_{ik}) g(\Theta_{ijk}) \exp\left[\lambda_3^3 (r_{ij} - r_{jk})^3\right],$$

$$g(\Theta) = 1 + \frac{c^2}{d^2} - \frac{c^2}{d^2 + (h - \cos \Theta)^2}.$$

Here r_{ij} is the distance between two atoms, and Θ_{ijk} is the angle between atomic bonds. The values for the parameters used in our calculations are $A = 1.849$ keV, $B = 0.487$ keV, $\lambda_1 = 2.480$ Å, $\lambda_2 = 1.736$ Å, $R = 2.7$ Å, $D = 0.3$ Å, $\alpha = 0$, $\beta = 4.357 \times 10^{-7}$, $n = 0.436$, $\lambda_3 =$

1.736 Å, $c = 1.015 \times 10^5$, $d = 17.51$, $h = -0.601$. They were obtained by optimizing the structure ($a_0 = 05.658$ Å [9]), elastic constants and bulk modulus of crystalline germanium (Table 1).

The Stillinger-Weber (SW) force-field model is defined as [5–7]

$$V(r_1, r_2, \dots, r_n, \Theta_1, \Theta_2, \dots, \Theta_m) = \frac{1}{2} \sum_{i,j} V_{ij} + \frac{1}{6} \sum_{i,j,k} V_{ijk},$$

$$V_{ij} = \varepsilon f_2\left(\frac{r_{ij}}{\sigma}\right),$$

$$V_{ijk} = \varepsilon f_3\left(\frac{\vec{r}_i}{\sigma}, \frac{\vec{r}_j}{\sigma}, \frac{\vec{r}_k}{\sigma}\right),$$

$$f_2(r) = \begin{cases} A(Br^{-p} - r^{-q}) \exp\left(\frac{1}{r-a}\right), & r < a \\ 0, & r \geq a \end{cases},$$

$$f_3(\vec{r}_i, \vec{r}_j, \vec{r}_k) = h(r_{ij}, r_{ik}, \Theta_{jik}) + h(r_{ji}, r_{jk}, \Theta_{ijk}) + h(r_{ki}, r_{kj}, \Theta_{ikj}),$$

$$h(r_{ij}, r_{ij}, \Theta_{jik}) = \lambda \exp\left(\frac{\gamma}{r_{ij} - a} + \frac{\gamma}{r_{ik} - a}\right) (\cos \Theta_{jik} - \cos \Theta_0)^2.$$

The original parameters from [6] have been used: $A = 7.049556277$, $B = 0.602245584$, $p = 4$, $q = 0$, $a = 1.8$, $\lambda = 31$, $\gamma = 1.2$, $\varepsilon = 1.93$ eV, $\sigma = 2.181$ Å, $\Theta_0 = 109.5^\circ$ (ideal tetrahedral angle).

Table 1. Calculated and experimental [10] values of elastic constants (C_{ij}) and bulk modulus (B_0) for crystalline diamond-type germanium.

Parameters (GPa)	Tersoff force-field	Stillinger-Weber force-field	Experiment [10]
C_{11}	128.9	117.8	128.8
C_{12}	48.4	61.2	48.3
C_{44}	67.1	43.1	67.1
B_0	75.3	80.1	75.1

The MD time step was 0.5 fs, the equilibration and production times were 20 ps each. As a result, 4000 atomic configurations were generated and used further for EXAFS signals calculation.

The Ge K-edge EXAFS signals were calculated for each configuration by the *ab initio* multiple-scattering code FEFF8 [11]. First, the scattering potentials and partial phase shifts were calculated only once for the cluster with the radius of 8 Å and centered at the Ge atom, i.e., for the equilibrium configuration, thus neglecting a variation of the scattering potentials due to thermal vibrations [3]. Next, the EXAFS signals $\chi(k)$ were calculated taking into account all MS contributions up to the eight order and with the half path length up to 6 Å that includes the contributions up to the fourth coordination shell. The complex exchange-correlation Hedin-Lundqvist potential, accounting for inelastic effects, and default values of muffin-tin radii ($R_{\text{mt}}(\text{Ge}) = 1.408 \text{ \AA}$), as provided within the FEFF8 code [11], were used. The position of the edge energy E_0 was fixed at the value optimized for the experimental EXAFS signal relative to the theoretical FEFF8 standard [2]. The Fourier transforms (FTs) of the EXAFS $\chi(k)k^2$ signals, multiplied by the 10% Gaussian window-function, were calculated in the k -space range from 3.5 \AA^{-1} to 17.5 \AA^{-1} . The FTs were not corrected by the backscattering amplitude and phase shift functions; therefore the positions of peaks in FTs do not correspond to the crystallographic values.

Similar EXAFS calculations were also performed for the equilibrium configuration, i.e., without any thermal disorder contribution. They allow one to reduce the number of non-equivalent multiple-scattering paths, which contribute in the R -space below 6 Å, to just 12 signals and to understand more easily the ranges of their significance both in k - and R -spaces.

3. Results and discussion

MD simulations instantly provide the Ge-Ge radial distribution functions (RDFs), which can be used to calculate the mean-square relative displacements (MSRDs) (known also as the Debye-Waller factors) for different coordination shells. This can be done by two approaches: one can (i) decompose the RDF into a set of Gaussian peaks and determine the MSRD values from the half-widths of the corresponding peaks or (ii) directly calculate the second moments of the RDF peaks when they do not overlap. In our case, the MSRD values obtained by the two methods for the first three coordination shells (Ge_1 , Ge_2 , Ge_3) around the absorbing germanium atom (Ge_0) (see Fig. 1) agree better than 0.0005 \AA^2 : the small difference is due to the slightly non-Gaussian shape of the RDF peaks.

The temperature dependences of the MSRDs determined within the two force-field models are compared with that obtained from the experimental EXAFS data [1, 2] in Fig.

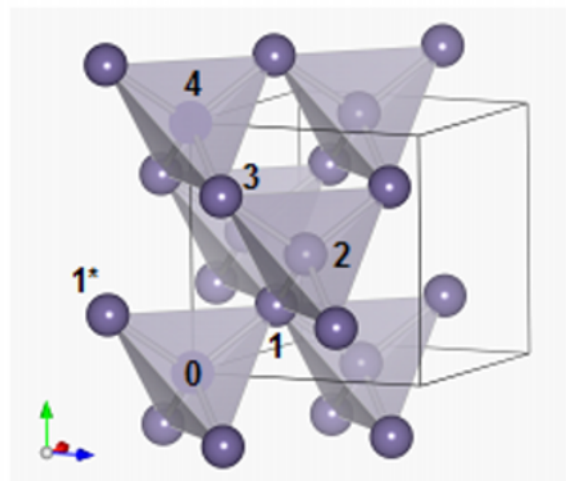


Figure 1. Crystallographic structure of diamond-type germanium. The coordination shell numbers, used in the description of the multiple-scattering paths, are shown.

2. For all three coordination shells the MD simulations predict smaller values of the MSRDs. The large differences at low temperatures ($T < 150 \text{ K}$) arise because the classical MD fails to account for quantum effects. In fact, the calculated MSRDs should grow linearly upon increasing temperature, as is indicated in Fig. 2 by solid lines. The lack of quantum effects in classical MD can be compensated by taking the result of the simulation performed at higher temperature. In our case, we found empirically that, for example, the EXAFS signal calculated with the SW potential at 395 K coincides very well with that measured at 300 K (see below).

From temperature dependences of the MSRDs, we concluded that for the current sets of force-field parameters the MSRDs values obtained from simulations using the Stillinger-Weber potential are closer to the experimental ones for the second and third shells, whereas for the first shell both models give close results being slightly below the experimental data. Therefore we will limit further our discussion to the results obtained by the Stillinger-Weber potential.

Multiple-scattering signals reflect the contributions from many-body distribution functions into the total EXAFS signal. In the absence of thermal disorder, i.e., for the equilibrium configuration, the number of the MS paths in such highly symmetrical material as diamond-type germanium is rather limited. In fact, there are only 12 signals (Fig. 3), corresponding to nonequivalent scattering paths, which contribute in the R -space below 6 Å, being the region of our interest. They involve the germanium

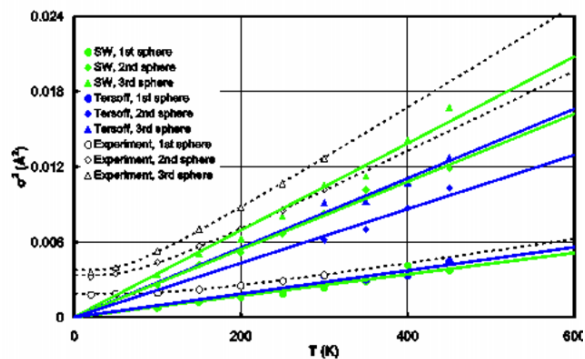


Figure 2. Temperature dependences of the MSRDs in the first (circles), second (diamonds) and third (triangles) coordination shells of germanium obtained for the SW and Tersoff force field models (solid symbols). The solid lines are linear approximations for the SW MSRDs. Experimental data (open symbols) and corresponding Einstein models (dashed lines) are taken from [1, 2].

atoms from the first four coordination shells (Fig. 1) and include four single-scattering (SS) paths (SS1–SS4), five double-scattering (DS) paths (DS1–DS5) and three triple-scattering (TS) paths (TS1–TS3) (Table 2). The SS signals dominate strongly for $k > 5 \text{ \AA}^{-1}$, whereas only the DS2 signal, a triangular path involving the atoms in the first and second coordination shells, has the highest amplitude among MS signals and therefore can be significant. The DS2 path contributes in Fourier transform mainly under the second peak at about 3.8 \AA (Fig. 3).

Table 2. Definition of the multiple-scattering paths (SS - single-scattering, DS - double-scattering, TS - triple-scattering) used in the Ge K-edge EXAFS calculations for the equilibrium configuration.

Scattering path	Path type	Path degeneracy	Half path length (Å)
0→1→0	SS1	4	2.4497
0→2→0	SS2	12	4.0004
0→1→1*→0	DS1	12	4.4499
0→1→2→0	DS2	24	4.4499
0→3→0	SS3	12	4.6908
0→1→0→1→0	TS1	4	4.8994
0→1→2→1→0	TS2	12	4.8994
0→1→0→1*→0	TS3	12	4.8994
0→1*→2→0	DS3	48	5.5705
0→1→3→0	DS4	48	5.5704
0→2→3→0	DS5	48	5.5704
0→4→0	SS4	6	5.6574

However, when thermal disorder is present, the crystal symmetry becomes broken, and the number of nonequiv-

alent scattering paths increases more than ten times as well as their interference becomes more complicated. This could influence the ratio between SS and MS signals, and thus requires a more rigorous analysis based on comparison of configuration-averaged EXAFS signals.

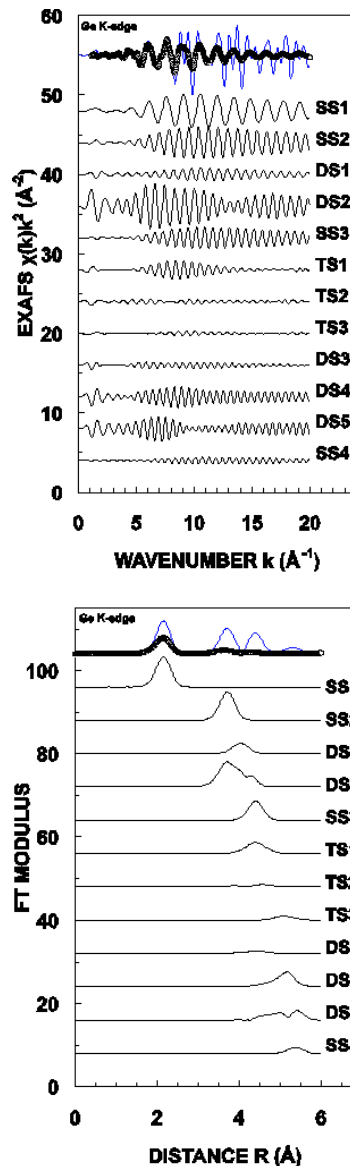


Figure 3. Comparison of the experimental [1] ($T = 300 \text{ K}$, open circles) and calculated for the equilibrium configuration (solid lines) Ge K-edge EXAFS $\chi(k)k^2$ signals (left panel) and their Fourier transforms (right panel). The difference between experimental and calculated signals is due to the absence of thermal disorder contribution in the simulation. The main single-scattering (SS), double-scattering (DS) and triple-scattering (TS) contributions are shown. The DS and TS contributions are multiplied by a factor 10 for clarity. The scattering path definitions are given in Table 2.

In Fig. 4 the configuration-averaged EXAFS signal $\chi(k)k^2$ for the Stillinger-Weber force-field model and its Fourier transform are compared with the experimental data from [1] at $T = 300$ K. As one can see, the contribution from the three coordination shells are overestimated due to the smaller value of the MSRD in the MD simulations at $T = 300$ K. To obtain the experimentally observed MSRD values at $T = 300$ K, one should perform the MD simulations at higher temperature to compensate the inaccuracy of the SW force-field model. By varying the temperature in the MD simulations, we found that the best agreement between experimental and calculated configuration-averaged EXAFS signals for the R-space range up to 6 Å can be obtained for the MD simulation performed at $T = 395$ K (Fig. 5).

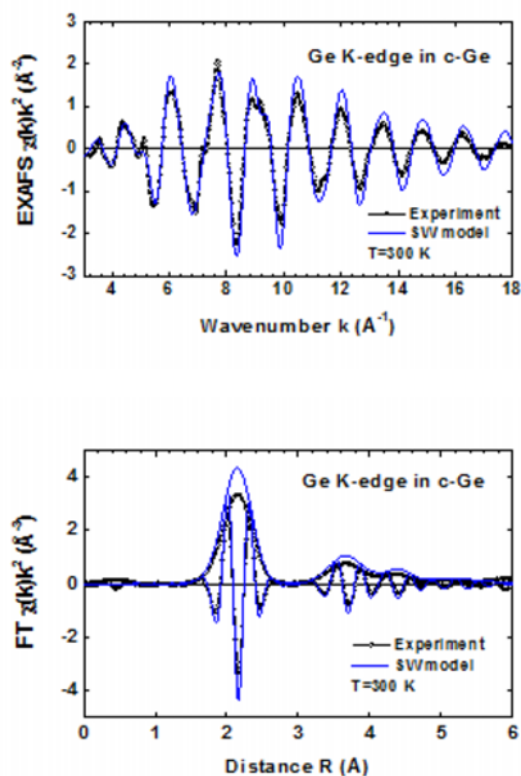


Figure 4. Comparison of the experimental [1] and configuration-averaged Ge K-edge EXAFS $\chi(k)k^2$ signals for SW force field model and their Fourier transforms at $T = 300$ K.

The perfect agreement between experimental and calculated EXAFS signals in Fig. 5 allows us to evaluate precisely the influence of the MS contributions in the presence of thermal disorder. It can be seen, that the MS

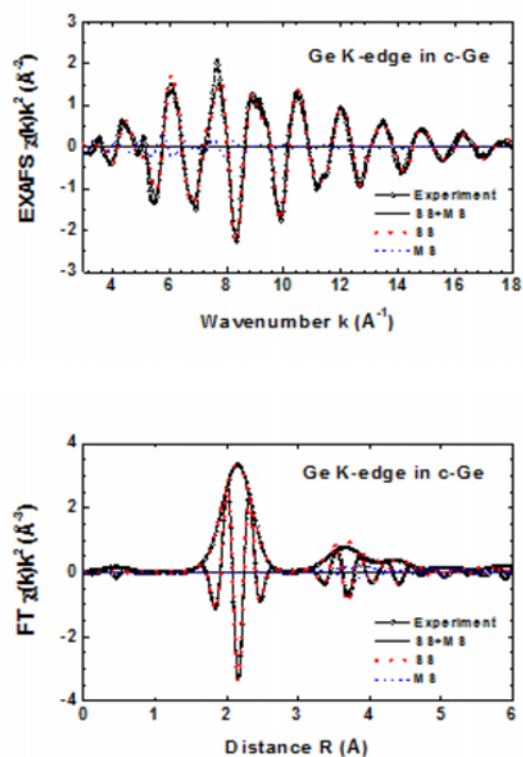


Figure 5. Experimental [1] ($T = 300$ K) and configuration-averaged ($T = 395$ K, up to 6.0 Å) Ge K-edge EXAFS spectra $\chi(k)k^2$ for SW force field model and their Fourier transforms. The single-scattering (SS) and multiple-scattering (MS) contributions are also shown. The MS effects contribute mainly at 3.8 Å and 5.0 Å.

effects contribute mainly at 3.8 Å and 5.0 Å. The MS contribution at 3.8 Å reduces the SS signal from the second coordination shell, whereas the MS contribution at 5.0 Å appears between the third and fourth shells. The temperature dependencies of the MS contributions in the range from 200 K to 400 K are shown in Fig. 6. It can be seen, that the MS signals are less sensitive to the thermal disorder compared to the SS contributions, therefore their relative importance increases upon temperature growth. As a result, one should be very careful when applying the single-scattering approximation for the EXAFS analysis in germanium, especially, at temperatures above 300 K.

4. Conclusions

In this work we have applied classical molecular dynamics (MD) simulations to the interpretation of the tempera-

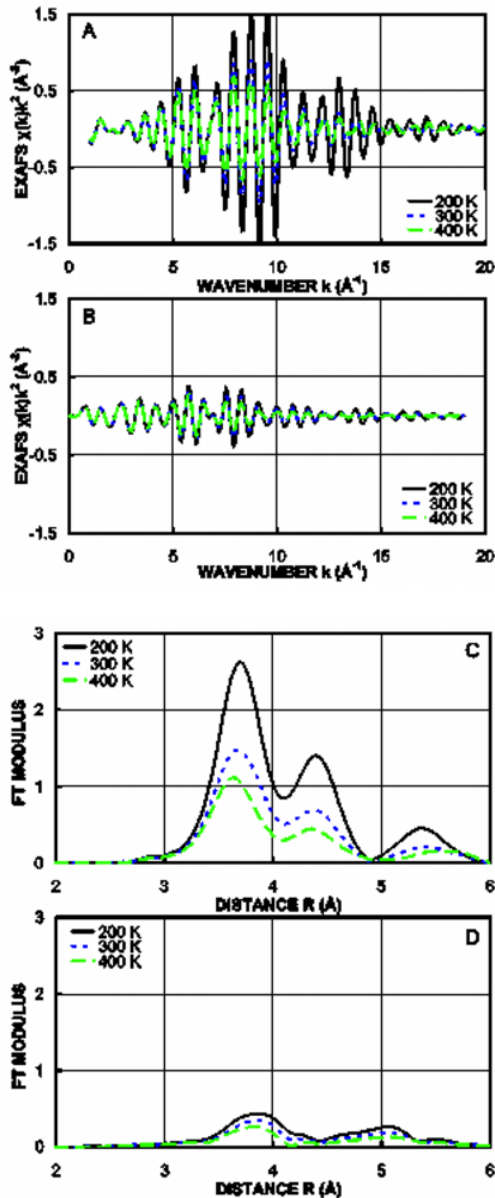


Figure 6. Configuration-averaged Ge K-edge EXAFS spectra $\chi(k)k^2$ in the range of the second and third coordination shells (a) and their Fourier transforms (FTs) (b), calculated in the temperature range from 200 K to 450 K. Multiple-scattering contributions to EXAFS spectra (c) and their FTs (d). The MS effects are less sensitive to the thermal disorder.

ture dependent Ge K-edge extended x-ray absorption fine structure (EXAFS) in crystalline germanium.

The Tersoff [4] and Stillinger-Weber (SW) [5–7] force-field models have been used in the MD simulations. It was found that the values of the mean-square relative displacements (MSRDs) obtained from simulations using the Stillinger-Weber (SW) potential are closer to the experimental ones [1, 2]. In fact, the MSRD values in the first coordination shell are rather well reproduced by both Tersoff [4] and Stillinger-Weber (SW) [5–7] models, but the SW potential provides better results for the second and third shells. Therefore, the SW potential was used in further configuration-averaged EXAFS calculations.

The influence of thermal disorder on the multiple-scattering (MS) contributions within the first four coordination shells has been evaluated. It was found that the MS effects mostly affect the contribution from the second coordination shell and are less sensitive to the thermal disorder compared to the single-scattering signals.

Acknowledgments

This work was supported by ESF Projects 2009/0202/1DP/1.1.1.2.0/09/APIA/VIAA/141, 2009/02021DP/1.1.1.2.0/09/AP1A/VIAA/044 and Latvian Government Research Grant No. 09.1518.

References

- [1] J. Purans et al., Phys. Rev. Lett. 100, 055901 (2008)
- [2] J. Purans et al., J. Phys. Conf. Ser. 190, 012063 (2009)
- [3] A. Kuzmin, R.A. Evarestov, J. Phys.-Condens. Mat. 21, 055401 (2009)
- [4] J. Tersoff, Phys. Rev. B 39, 5566 (1989)
- [5] F.H. Stillinger, T.A. Weber, Phys. Rev. B 31, 5262 (1985)
- [6] K. Ding, H.C. Andersen, Phys. Rev. B 34, 6987 (1986)
- [7] M. Posselt, A. Gabriel, Phys. Rev. B 80, 045202 (2009)
- [8] J.D. Gale, A.L. Rohl, Mol. Simulat. 9, 291 (2003)
- [9] A. Smakula, J. Kalnajs, Phys. Rev. B 99, 1737 (1955)
- [10] J.C. Noya, C.P. Herrero, R. Ramírez, Phys. Rev. B 56, 237 (1997)
- [11] A.L. Ankudinov, B. Ravel, J.J. Rehr, S.D. Conradson, Phys. Rev. B 58, 7565 (1998)